Article

Determining the Location of the UAV When Flying in a Group

Milan Džunda [ID], Peter Dzurovčin [ID], Sebastián Čikovský * and Lucia Melníková

Department of Air Traffic Management, Faculty of Aeronautics, Technical University of Kosice,
040 01 Kosice, Slovakia; milan.dzunda@tuke.sk (M.D.); peter.dzurovcin@tuke.sk (P.D.);
lucia.melnikova@tuke.sk (L.M.)
* Correspondence: sebastian.cikovsky@tuke.sk

Abstract: This paper created a flight trajectory model of five uncrewed aerial vehicles (UAVs) in the geocentric coordinate system, provided the UAVs fly in the specified formation. Based on this model, equations for determining the position of a selected member of a group of UAVs were created, provided that the group communicates with each other in its telecommunications network. The simulation confirmed that if we know the exact coordinates of the four member UAVs of the group and their distances from the leader of the group, then the mean value of the error in determining its position in flight is equal to 0.044 m, and the variance is equal to 2.9 m^2. We consider these errors to be methodological errors of the proposed method. Next, we checked how the error of determining the position of the group leader depends on the distance measurement errors between the individual UAVs and the group leader. The simulation confirmed that if errors in measuring the distance between individual UAVs and the group leader are from 0.01 m to 12.0 m, the mean values of group commander position determination errors range from 0.11 m to 34.6 m. The simulation result showed that to accurately determine the group commander's position, the distance measurement errors between individual UAVs and the group commander must be less than 1.9 m. The research results showed that the telemetry method can be used to determine the position of individual members of the UAV group. The advantage of this method is that it does not require the reception of signals from satellite navigation systems, which can be interfered with under certain conditions. The disadvantage of the method is the need to synchronize the time bases of individual UAVs that communicate in the telecommunications network.

1. Introduction

Published works on UAV systems confirm that these systems currently have a wide range of applications. UAV systems can be used for terrain monitoring to protect state borders, for terrain scanning in agriculture, in the military for reconnaissance and attack missions, for monitoring important objects, etc. The advantage of using UAVs is their low price, relative autonomy in the activities performed, and the possibility of multiple use [1,2]. The increased demand for UAVs results from the increasingly complex environment of the performed reconnaissance and monitoring missions. A significant problem is represented by monitoring tasks that require high performance in terms of autonomous orientation and communication in the space of the ongoing mission. However, a single UAV can hardly meet its actual task requirements because its sensor's field of view can be easily blocked, limiting its ability to perform tasks [3]. The cooperation of several drones should eliminate these situations and ensure more accessible and stable monitoring of the area. Currently, multi-UAV collaborative planning using the artificial potential field method, bionic algorithm, or control algorithm is analyzed in [4,5]. In the case of using the artificial potential field method for collaborative planning, it is possible to slip into local optimality. Then, it is challenging to create a mathematical model of UAV trajectories. In the case of ant

colony and particle swarm bionic algorithms, it is difficult to satisfy the real-time demand due to their limited processing efficiency [6,7]. Animesh Sahu [8] and others created a study on object movement tracking using UAVs in two dimensions based on a predictive control algorithm model. The model is based on the Gaussian Process (GP), which combines the hyperparameters used in the predictive control phase and significantly impacts mission efficiency. A comprehensive analysis of the above research found that most current research on multi-UAV trajectory planning through cooperative formation has been conducted in two-dimensional space. This results in limitations, such as the computational complexity of the large-scale model and the long time for real-time computation. At the same time, current research needs help in creating a complete non-linear 3D movement model of the UAV, which results in difficulty in meeting the actual requirements related to the mission objective [9]. As for the traditional multi-UAV sensors, their working areas need to be improved. Low data formation and retention capabilities prevent them from becoming a hot candidate for use in this field [10]. Multi-UAV formations, control, communication, and computer processing of time data must be complemented by distributed control strategies, which present higher requirements for the multi-UAV formation. A typical multi-UAV system is a multi-agent system [11]. The user can measure the relative distance from the neighboring user and guide the controlled shift to the next UAV. In this way, the desired formation can be achieved. There needs to be more control of their mutual positions. Because of this, they do not have the same sense of direction. There are also many studies on the cooperative creation of UAV control [12,13], which provide path planning, optimal perceptual geometry, distributed control law design, and information architectures. Multi-UAV cooperative trajectory planning (MUCTP) is planning multiple safe and collision-free flight trajectories based on the spatial location of UAVs, mission points, and obstacles in a complex planning environment [14,15]. The planned trajectory of a single UAV can hardly handle complex missions due to its limited maneuverability and payload. MUCTP has the advantage of being more flexible and efficient in carrying out missions than standalone UAV assets. For this reason, when performing complex missions, this solution is gradually replacing using separate UAVs. However, MUCTP also increases the difficulty of planning the trajectory of UAVs. In cooperative planning, the self-constraints of heterogeneous UAVs and the mutual constraints between multiple UAVs may lead to conflicting relationships and disturbances between each UAV and the mission point, ultimately leading to mission failure [16,17].

In recent years, to improve the efficiency of MUCTP scheduling, researchers have proposed many algorithms that have shown good performance in solving MUCTP problems, and these algorithms are mainly divided into three categories:

- Cooperative trajectory planning based on intelligent optimization algorithms
- Cooperative trajectory planning based on reinforcement learning
- Cooperative trajectory planning based on the spline interpolation algorithm

Based on the algorithms presented in [17], it is possible to design the architecture of an anti-collision system for UAVs that can determine the position of the UAV relative to other users in the air communication network. The condition for the functioning of these algorithms is that all flying objects communicate with each other. The results of the research work on the anti-collision system with the radar obstacle detector are discussed in [18]. The main tasks set for this system are detection of static and moving obstacles, estimation of the distance between the flying object and the obstacle, and their relative speed. Most cooperative obstacle avoidance strategies use Wmethod. The APF method [19,20] is widely used in the design of anti-collision systems for cooperative UAV formations. The algorithm relies on the creation of gravitational and repulsive fields to calculate the resultant force that determines the path planning at each moment. However, if the chosen design of the field function is incorrect, the APF algorithm may fall into the local optimal solution. Another disadvantage of the implementation of this method is the fact that it does not take into account the limitations of the dynamic movement of the UAV, which makes it difficult to track the planned path in real time. Based on the research of Xianyong et al. [21],

an improved deep deterministic policy gradient (DDPG) algorithm was proposed. They modified the UAV model and processed empirical data based on the vector distance to improve computational efficiency. The DDPG contains several hyperparameters and is sensitive to these parameters. For this reason, it takes a relatively long time for the parameters to be adjusted during the algorithm testing phase. The double-delayed policy gradient algorithm (TD3) [22], which is based on the DDPG, optimizes the input value of the overestimation problem. This improvement makes the TD3 perform better than the DDPG in many tasks. In [23], a TD3-based UAV navigation algorithm is proposed to enable UAVs to perform navigation tasks in a dynamic environment with multiple obstacles. Zhang [24] proposed a decision-making method using deep neural networks. They obtained samples by constructing various maneuvers and simulations, trained a deep neural network to predict the situation, and designed a situation evaluation function and optimal action selection. Luo [25] used a dynamic Bayesian method and made full use of the previous experience of aerial combat in the battlefield situation to construct a decision network to realize effective sensing and orientation in the research area. These methods have shortcomings in solving the problem of monitoring and cooperative air combat of UAVs.

The technological level of fully autonomous unmanned UAVs has advanced rapidly in recent years and, similar to many other aviation technologies, is poised to transform from purely military equipment into a reliable new technology for civilian use. The article considers using a fully autonomous formation of selected UAV assets above 150 kg. According to the currently valid legislation in the European Union and Slovakia, if the weight of the selected UAV device is greater than 20 kg, it is subject to registration at the transport office and the requirement for insurance. The person who controls the unmanned aircraft must have issued a decision on determining the conditions of safe operation for unmanned aircraft according to Section 7 of the Aviation Act. Moreover, such a flight is significantly limited by a maximum height of 120 m above ground level and a distance of no more than a kilometer from the person who controls it. UAVs can only fly in uncontrolled airspace. Uncontrolled airports can also be found on the air map. Uncontrolled aerodrome zones are established around these airports, extending horizontally up to a distance of 5.5 km from the airport reference point and up to a height of 4000 ft AMSL. In this area, observing the maximum flight height established for uncontrolled airspace is optimal. Still, it is possible to fly here only based on flight coordination with the airport operator. In our case, we consider the flight of autonomous UAVs in a specified formation from the weight category above 150 kg. For this reason, we will not consider the legislative restrictions resulting from Act No. 143/1998 Coll. on civil aviation. The Transport Office based on this Act and Decision No. 2/2019 from 14 November 2019 prohibits the flight of an autonomous aircraft and an unmanned aircraft with a maximum take-off weight greater than 150 kg in the airspace.

In this work, we present the procedure for creating a model of the trajectories of five UAVs in our chosen set-up. We assume that the flight trajectories of UAVs are modeled in the geocentric coordinate system (ECEF—Earth-centered, Earth-fixed). The creation of the model requires the derivation of the movement equations of five UAVs in the chosen coordinate system and the assembly we selected. Our chosen set-up consists of five UAVs, including the commander. When creating the model of the UAV flight trajectories, we assumed that the developed models would be used to verify the accuracy of the navigation of the UAVs that fly in the specified formation. Therefore, we designed the flight trajectories of five UAVs, which consist of a straight flight section and several curvilinear flight sections. In the next part of the work, we investigated the possibilities of determining the position of UAVs that fly in the selected assembly, using the telemetry method with an emphasis on the accuracy of determining the position of the UAV in the assembly. All simulations were performed using MATLAB R2023a software. Using the performed simulation, the accuracy of determining the position of the group commander using the telemetry method was verified, and the possibilities of using the proposed method to control the movement

of the UAVs in the selected assembly were evaluated We chose the Sliač airport reference point as the starting point for the beginning of the simulated flight.

2. Materials and Methods

This section presents the methodology for creating a model of the flight trajectory of a group of five UAVs that fly in a specified formation. Furthermore, using the created model, equations for determining the position of the selected assembly member were derived, and the accuracy of determining its position was evaluated. We assumed that a group of five UAVs works in a telecommunications network created for the assembly's flight control needs.

2.1. Flight Trajectory Model of a Group of Five UAVs

To verify the accuracy of determining the position of individual members of the group of UAVs working in the communication network, it was necessary to create a model of their flight trajectory. These UAV movement models provide us with information about their position in space. In developing the models, we have abstained from the forces' influence on the UAV during the flight. We assume that this approximation is relevant for verifying the accuracy of determining the position of the selected member of the group.

In Figure 1, ZP_V is the initial position of the leader of the group of UAVs, and ZP_i, i = 1, 4 are the initial positions of the members of the group of UAVs, 1 to 4. Other group members, at designated distances for the flight duration, follow the group leader. Based on data from other UAVs, other group members determine its position. The co-ordinates of the initial position of the members of the UAV group are shown in Table 1. When creating a model of the movement of five flying UAVs, they chose the formation they would fly in. At the head of the formation is the leader of the group, and to its left and right sides are two UAVs. In developing the model, a condition was observed that the maximum distance between the group's leader and any group member should not exceed 1000.0 m. We assumed that the group would form in the surrounding area of the Sliač airbase and fly eastward at an altitude of 1850.0 m. The initial position of the group is shown in Figure 1. The distance between group members is at least 300.0 m.

We assumed that these coordinates are considered to be the reference and represent the start point of the flight trajectory, Xp_i, where Xp_i [xp_i, yp_i, zp_i]. When modeling the movement of a group of UAVs, we set the condition that this group's flight trajectory will contain one rectilinear section and three curvilinear sections in the shape of a circle.

We can set the initial parameters of the flight modeling of five UAVs by the task solved by the UAV group. The parameters of the models that can be entered are the initial positions of the UAV, the time of rectilinear flight, and flight, in turn, including its radius. Another requirement for the motion models was to determine and visualize the positions of the UAV in the ECEF rectangular coordinate system. The positions of the UAV must be determined according to the selected period by x, y, and z coordinates, in meters.
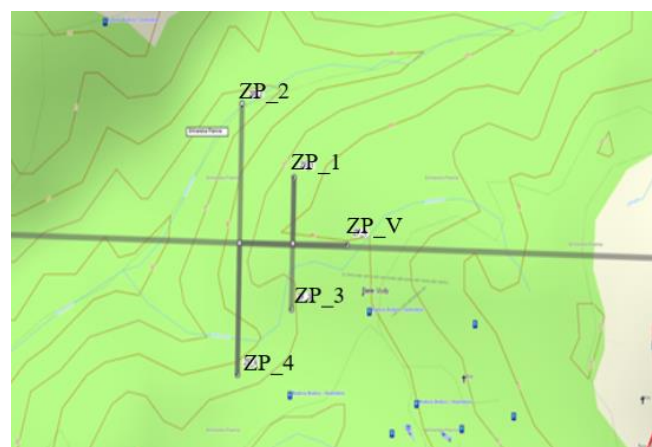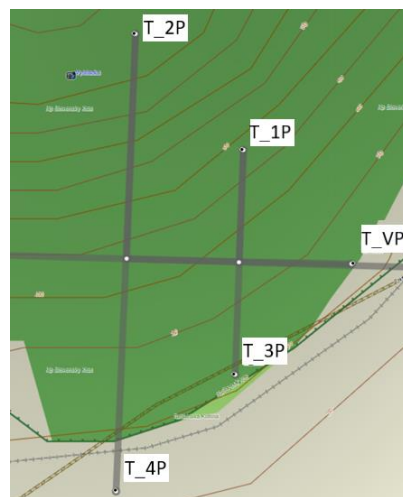

Figure 1. Initial position of the UAV group.

Table 1. Coordinates of the initial positions of the group of UAVs.

UAV Marking	Coordinates WGS 84	MSL, m	Flight Height, m	Coordinates JTSK		
				X, km	Y, km	Z, km
ZP_V	N48 37 43.5 E19 37 09.2	905	1850.0	3979.461	1418.527	4764.761
ZP_1	N48 37 53.4 E19 36 54.6	884.0	1850.0	3979.345	1418.168	4764.963
ZP_2	N48 38 03.9 E19 36 40.7	814.0	1850.0	3979.211	1417.818	4765.177
ZP_3	N48 37 34.0 E19 36 53.9	865.0	1850.0	3979.774	1418.306	4764.567
ZP_4	N48 37 24.4 E19 36 39.1	844.0	1850.0	3980.085	1418.095	4764.371

In Figure 2, T_VP is the position of the leader of the group of UAVs, and T_iP, i = 1, 4 are the positions of the members of the group of UAVs, 1 to 4. The coordinates of the positions of the UAV group members at the end of a rectilinear flight are provided in Table 2. The motion model of the initial flight phase of five UAVs (rectilinear flight) was created based on these assumptions. We assumed a straight flight at an altitude of 1850.0 m. The initial coordinates of the five UAVs are shown in Table 1. When creating the flight trajectory model, we used knowledge from our previous works [26]. We assumed a rectilinear flight throughout the line, which can be described by the equation of a line in a three-dimensional space. The line in the space is provided by two points or one point and a direction vector. Line Xk XP may be defined as follows: the line goes through the starting point Xp_i $[xp_i, yp_i, zp_i]$ and the final point Xk_i $[xk_i, yk_i, zk_i]$. The endpoint coordinates are presented in Figure 2 and Table 2.

Figure 2. Group positions at the end of a rectilinear flight.

Table 2. Coordinates of the positions of UAV group members at the end of a rectilinear flight.

UAV Marking	Coordinates WGS 84	MSL, m	Flight Height, m	Coordinates JTSK		
				X, km	Y, km	Z, km
T_VP	N48 36 25.4 E20 44 14.5	253.0	1850.0	3952.715	1496.553	4763.165
T_1P	N48 36 35.3 E20 44 00.1	367.0	1850.0	3952.605	1496.196	4763.368
T_2P	N48 36 45.3 E20 43 46.0	580.0	1850.0	3952.396	1496.093	4763.572
T_3P	N48 36 15.9 E20 43 59.0	247.0	1850.0	3953.034	1496.334	4762.971
T_4P	N48 36 05.9 E20 43 43.4	236.0	1850.0	3953.364	1496.117	4762.767

For the directional vector $\bar{U}_i$, we express it in the form:

$$\bar{U} = Xk_i - Xp_i = [xk_i - xp_i; yk_i - yp_i; zk_i - zp_i];$$
$$\bar{U} = [u_{1i}; u_{2i}; u_{3i}]; \ i = 1, 5. \tag{1}$$

Then, a parametric expression of the line $Xp\ Xk$ has the form:

$$x_i = xp_i + t.u_1\ ;\ y_i = yp_i\ +\ .u_2\ ;\ z_i = zp_i + t.u_3\ ;$$
$$t \in \langle 0,\ 1 \rangle, \tag{2}$$

where $\mathbf{Xp_i}\ [xp_i\ , yp_i\ , zp_i\ ]$ is the starting point of the flight trajectory, $\mathbf{Xk_i}\ [xk_i\ , yk_i\ , zk_i\ ]$ is the endpoint of a straight-line flight path, and t is the length of the step of the flight trajectory. When constructing models of five UAVs, we can choose the endpoint of the flight trajectory as desired according to the nature of the task being solved. In Figure 3, the initial points of the flight trajectory of individual UAVs are marked with + symbols and V or 1 to 4. The endpoints of the rectilinear flight of individual UAVs are marked with a + sign of a different color. The symbols * and ° indicate the beginning and end of the turn. Subsequently, we created models of UAV flight trajectories, formed by three turns. The models were created assuming that all UAVs fly at a constant altitude. We modeled the turns using circle shapes. The letter r denotes the radius of the circle. We assumed that the radius r must be in line with the maneuverability of the UAV.
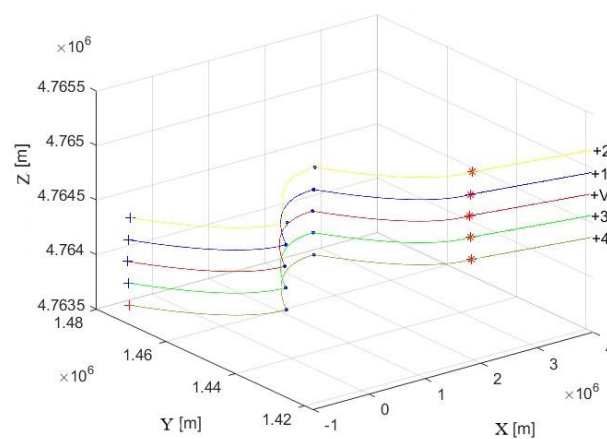

Figure 3. Results of the simulation of flight trajectories of five UAVs.

If we have point S [x; y] = S [0; 0], it applies to all points on the circle:

$$x^2 + y^2 = r^2 \tag{3}$$

If the point S is determined as $S[x;\ y;\ z] = S\ [0;\ 0;\ 0]$, then the implicit expression of the circle is:

$$x^2 + y^2 - r^2 = 0;\ z = 0; \tag{4}$$

We express the parametric equations of this circle as follows:

$$x = r.\cos(t);\ y = r.\sin(t);\ z = 0;\ t \in \langle 0,\ 2\pi \rangle \tag{5}$$

When creating models of curvilinear flight trajectories of the five UAVs, we assumed that the center of rotation of the flying object was at the point $Xk_i\ [xk_i\ , yk_i\ , zk_i\ ]$ and $zk_i = $ constant. We express the parametric equations of such a circle as follows:

$$x_i = r.\cos(t_i) + xk_i;\ y_i = r.\sin(t_i) + yk_i;$$
$$zk_i = \text{const.};\ t \in \langle 0,\ 2\pi \rangle; \tag{6}$$

with Equation (6), the modeling of curvilinear flight trajectories of five UAVs was performed.

Simulation Results

The results of the simulation of the flight trajectories of the five UAVs are shown in Figure 3. The initial positions of the individual UAVs are marked with a + sign. The leader of the group is marked V. The other members of the group are marked with numbers 1 to 4.

The endpoints of the flight trajectories of the five UAVs are marked with + signs of different colors. From Figure 3, it is clear that the flight trajectories of the five UAVs are composed of four parts.

In Figure 4, details of the simulation of the flight trajectories of the five UAVs in the first turn are shown. It is clear from the picture that the UAVs flew in a set formation and kept the specified distances between them.
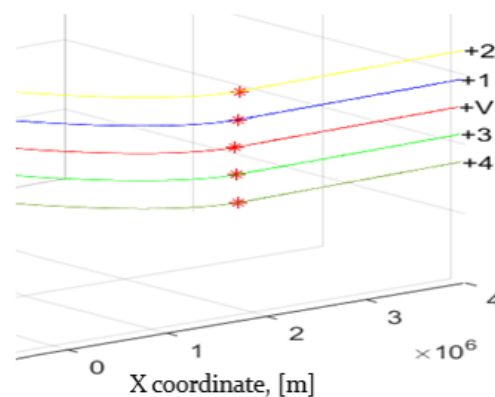

Figure 4. Details of the simulation of the flight trajectories of the five UAVs in the first turn.

A detailed simulation of the flight trajectories of the five UAVs in the second and third turns is shown in Figures 5 and 6.
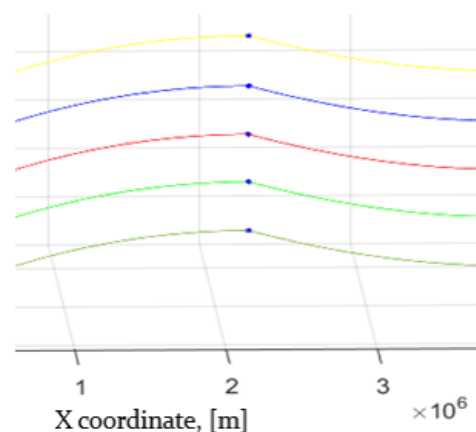

Figure 5. Details of the simulation of the flight trajectories of the five UAVs in the second turn.

The model of the straight flight section was provided by Equations (1) and (2). The curvilinear flight model was provided by Equations (5) and (6). During the simulations, the parameters of the UAV trajectories were chosen to correspond to the flight of the General Atomics MQ-9 Reaper UAV. The flight speed was around 310 km.h^{-1}, corresponding to 86.1 m.s^{-1}. The height of the flight was equal to 1850.0 m due to the rugged terrain over which the UAV group was flying. The simulation results confirmed that the created models are suitable for simulating the flight of a group of five UAVs in the selected set-up. Among the main advantages of the mentioned flight model of five UAVs in a group is the model's simplicity and the high speed of simulation.
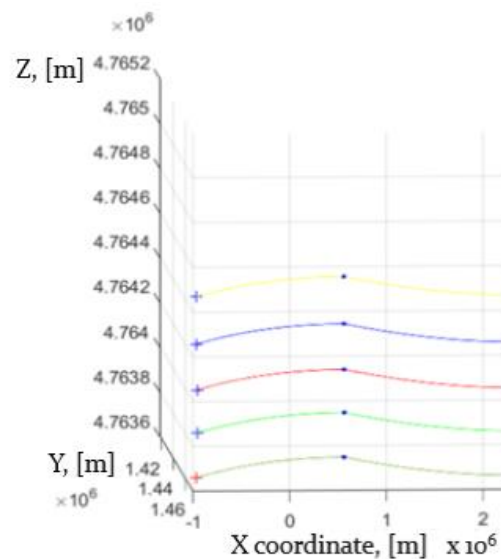
Figure 6. Details of the simulation of the flight trajectories of the five UAVs in the third turn.

2.2. Model of the Communication Network of a Group of UAVs

The designed model assumes that all UAVs operate in the communication network, and each UAV transmits information on its position. A prerequisite of the flight control of a UAV group is that the communication network must be synchronized. Every UAV is assigned a strictly specified time for transmitting communication messages. Designing the communication network, we started from the fact that if we know the location of a minimum of four points in space and the distances of these points from an unknown point, we can calculate the position of the unknown point. We presupposed that based on the message transmission by individual UAVs, each UAV will be able to measure distances from those users because individual users will provide times of communication message transmissions. This method of position determination is a designated telemetric method. The principle of the telemetric method is described in detail in [27].

We assumed that all UAVs work in the communication network (see Figure 7) and transmit in short time intervals, among other things, messages on their positions. The time of signals spreading between the UAV's transmitter ZP_i, i = 1 to 4, and the group leader's receiver ZP_V is directly proportional to the distance between them. Measuring the distances, d_i-v, i = 1 to 4, between UAVs ZP_i and the group leader ZP_V, it possible to determine the group leader's location if we know the positions of the individual UAVs. The position of the group leader ZP_V against other users of communication network ZP_i, i = 1 to 4 is demonstrated in Figure 7.

On the condition that we have identified the coordinates of individual users of the aviation communication network, ZP_i, (x_i, y_i, z_i) i = 1 to 4, and the distances, $d_{i\text{-}v}$, i = 1 to 4, of the group leader's receiver, ZP_V, from those users, we can determine its position with the coordinates (x, y, and z). The distances, $d_{i\text{-}v}$, i = 1 to 4, of the group leader's receiver, ZP_V, from users ZP_i, i = 1 to 4, will be determined according to the relationship:

$$d_{i-v} = \sqrt{(x - x_i)^2 + (y - y_i)^2 + (z - z_i)^2}, \text{ where } i = 1, 2, 3, 4. \tag{7}$$

If the user ZP_i, i = 1 to 4 sends the message at time t_i, the message will be received at time t_p. Provided that the speed of electromagnetic waves' spreading (c) is known, the distance between the source of transmission, ZP_i, i = 1 to 4, and the group leader's receiver, ZP_V, $d_{i\text{-}v}$, is as follows:

$$d_{i-v} = c(t_{pi} - t_i) = c\tau_i, \text{ where } i = 1, 2, 3, 4. \tag{8}$$

In reality, the calculated distance is burdened with some errors. For that reason, the distance is denoted pseudo-distance. If the time base of the group leader's receiver, ZP_V, is shifted by an unknown time interval, Δt, then this interval can be converted to a distance, b, using the equation:

$$b = c.\Delta t \tag{9}$$

The actual distance, then, will be equal to:

$$D_i = d_{i-v} - b, \tag{10}$$

where: i = 1, 2, 3, 4, d_(i-v) is the measured pseudo-distance, D_i is the actual distance, and b is the error of the distance measurement. The delay, Δt, causes a distance, D_i, measurement error due to a shift in the time bases of the UAVs and the group leader's receiver, ZP_V.
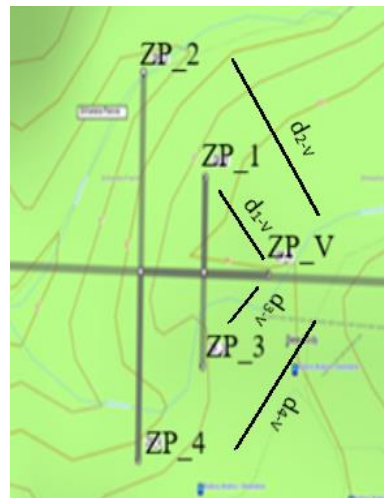

Figure 7. Positions of the individual UAVs in the group.

2.3. Equations for Determining the Location of a Selected Member of a Group of UAVs

The unknown coordinates of the group leader's receiver, ZP_V, include the unknown b, and to calculate the position ZP_V, we need four equations of the following form:

$$(d_{i-v} - b) = c.(\tau_i - \Delta t) = \sqrt{(x - x_i)^2 + (y - y_i)^2 + (z - z_i)^2} \tag{11}$$

where i = 1, 2, 3, and 4.

After adjustments, we obtain:

$$(x - x_i)^2 + (y - y_i)^2 + (z - z_i)^2 - (d_{i-v} - b)^2 = 0, \text{ where } i = 1, 2, 3, 4 \tag{12}$$

x, y, z—position of the group leader's receiver, ZP_V,

d_{i-v}—measured pseudo-distance from the group leader's receiver, ZP_V, to the i-th UAV,

τ_i—time of the signal spreading from the i-th UAV to the group leader's receiver, ZP_V (x, y, z),

Δt—time interval by which the receiver's time base is shifted,

b—shift of the receiver's time base converted into distance.

The position of the group leader's receiver, ZP_V, will be expressed through 4 equations in 4 unknowns:

$$(x - x_i)^2 + (y - y_i)^2 + (z - z_i)^2 - (d_{1-v} - b)^2 = 0, \tag{13}$$

$$(x - x_2)^2 + (y - y_2)^2 + (z - z_2)^2 - (d_{2-v} - b)^2 = 0, \tag{14}$$

$$(x - x_3)^2 + (y - y_3)^2 + (z - z_3)^2 - (d_{3-v} - b)^2 = 0, \tag{15}$$

$$(x - x_4)^2 + (y - y_4)^2 + (z - z_4)^2 - (d_{4-v} - b)^2 = 0, \tag{16}$$

where d_{1-v}, d_{2-v}, d_{3-v}, and d_{4-v} are the measured pseudo-distances from ZP_1-4 to the group leader's receiver, ZP_V, and:

x_1, y_1, z_1—coordinates of the UAV ZP_1,
x_2, y_2, z_2—coordinates of the UAV ZP_2,
x_3, y_3, z_3—coordinates of the UAV ZP_3,
x_4, y_4, z_4—coordinates of the UAV ZP_4,
x, y, z—coordinates of the group leader's receiver, ZP_V,
b—shift of the group leader's receiver's, ZP_V, time base converted to distance.

Subtraction of (16) from (13) is valid, as follows:

$$f_{14} = x_{14}x + y_{14}y + d_{41}b + e_{14} \tag{17}$$

Subtraction of (16) from (14) is valid, and it holds that:

$$f_{24} = x_{24}x + y_{24}y + z_{24}z + b_{42}b + e_{24} \tag{18}$$

Subtraction of (16) from (15) is valid, as follows:

$$f_{34} = x_{34}x + y_{34}y + z_{34}z + d_{34}b + e_{34} \tag{19}$$

If the variable b is considered constant (the so-called factor of homogenization), then, depending on Expressions (17)–(19), a system of three equations with three unknown variables is obtained. The method of resultants of the multi-polynomials has been applied to solve the system of linear equations: $x = g(b)$, $y = g(b)$, $z = g(b)$ [27].

Then, the following applies:

$$f_1 = (x_{14}x + d_{41}b + e_{14})k + y_{14}y + z_{14}z \tag{20}$$

$$f_2 = (x_{24}x + d_{42}b + e_{24})k + y_{24}y + z_{24}z \tag{21}$$

$$f_3 = (x_{34}x + d_{43}b + e_{34})k + y_{34}y + z_{34}z \tag{22}$$

If the variable "k" turns into the factor of homogenization, Jacobi's determinant of the coordinate *x* by (20)–(21) is expressed as:

$$\mathbf{J}_x = det \begin{pmatrix} \frac{df_1}{dy} & \frac{df_1}{dz} & \frac{df_1}{dk} \\ \frac{df_2}{dy} & \frac{df_2}{dz} & \frac{df_2}{dk} \\ \frac{df_3}{dy} & \frac{df_3}{dz} & \frac{df_3}{dk} \end{pmatrix} \tag{23}$$

In compliance with (20)–(22), $y = g(b)$ is valid:

$$f_4 = (y_{14}y + d_{41}b + e_{14})k + x_{14}x + z_{14}z \tag{24}$$

$$f_5 = (y_{24}y + d_{42}b + e_{24})k + x_{24}x + z_{24}z \tag{25}$$

$$f_6 = (y_{34}y + d_{43}b + e_{34})k + x_{34}x + z_{34}z \tag{26}$$

Jacobi's determinant for the coordinate *y* is expressed as:

$$\mathbf{J}_y = det \begin{pmatrix} \frac{df_4}{dx} & \frac{df_4}{dz} & \frac{df_4}{dk} \\ \frac{df_5}{dx} & \frac{df_5}{dz} & \frac{df_5}{dk} \\ \frac{df_6}{dx} & \frac{df_6}{dz} & \frac{df_6}{dk} \end{pmatrix} \tag{27}$$

In compliance with (20)–(22), $z = g\,(b)$ is valid:

$$f_7 = (z_{14}z + d_{41}b + e_{14})k + x_{14}x + y_{14}y \tag{28}$$

$$f_8 = (z_{24}z + d_{42}b + e_{24})k + x_{24}x + y_{24}y \tag{29}$$

$$f_9 = (z_{34}z + d_{43}b + e_{34})k + x_{34}x + y_{34}y \tag{30}$$

Jacobi's determinant for coordinate z is expressed as:

$$\mathbf{J}_z = det \begin{pmatrix} \frac{df_7}{dx} & \frac{df_7}{dy} & \frac{df_7}{dk} \\ \frac{df_8}{dx} & \frac{df_8}{dy} & \frac{df_8}{dk} \\ \frac{df_9}{dx} & \frac{df_9}{dy} & \frac{df_9}{dk} \end{pmatrix} \tag{31}$$

From Expressions (23), (27), and (31), the value of the determinants J_x, J_y, and J_z has been obtained. The variable equations: $x = g(b)$, $y = g(b)$, $z = g(b)$, by applying the value of each determinant, are the results. Substituting the expression for x, y, and z into Equation (13), the quadratic function for the unknown variable b is obtained:

$$Ab^2 + Bb + C = 0 \tag{32}$$

Solutions of the quadratic Equation (32) have two roots, b+ and b−. We calculate the coordinates of the P (x+, y+, z+) and P (x−, y−, z−). To come to the correct solution, we calculate the norm:

$$norm = \sqrt{x^2 + y^2 + z^2} \tag{33}$$

for (x, y, z) b− and (x, y, z) b+. If the coordinates of the receiver are fed into the coordinate reference system, the norm of the position vector will be close to the value of the radius of the Earth (Re = 6372.797 km), and this solution for P (x, y, z) will be regarded as a correct one [27].

2.4. The Accuracy of Determining the Position of the Selected Member of the Group When Flying in a Group of UAVs

According to Equations (1)–(33), the flight of a group of five UAVs was simulated, and the accuracy of determining the position of the selected group member was evaluated. We were interested in whether using the telemetry method would make it possible to determine the position of individual UAVs and use the position determination results to control the flight of UAVs in a group. It was intended that UAVs work in the telecommunications network, as stated in the introduction of this section (see Figure 7). The positions of the individual UAVs and the group's flight simulation results are presented in the first section. We investigated how accurately it is possible to determine the position of the group commander using the telemetry method. First, the accuracy of the telemetry method of determining the position of the ZP_V group commander was verified, assuming that we know the positions of the individual UAVs (see Figure 1), ZP_i, i = 1 to 4, and the distances between the individual UAVs and the group commander. The simulation results are shown in Table 3. ZP_V are the coordinates of the group commander, and ZP_VS are the coordinates of the group commander determined by the telemetric method.

Table 3. Coordinates of the group commander of the UAVs.

Name	Coordinates of the Group Commander of the UAVs		
	X, m	Y, m	Z, m
ZP_V	3,979,461.0	1,418,527.0	4,764,761.0
ZP_VS	3,979,461.0	1,418,527.0	4,764,761.0

As seen from Table 3, the simulation results confirmed that the telemetric method allows for determining the location of individual members of the group, provided that all members of the group work in the telecommunications network. A prerequisite for the exact determination of the position of, for example, the group commander, is that its receiver has the exact coordinates of the position of the other group members available. It is also necessary to know the exact values of the distance between the group commander and the individual members of the UAV group. In real life, we often encounter cases where the operation of the communication network can be intentionally disrupted by interference, or the synchronization in the communication network is unstable. This can cause errors in measuring the distance between individual members of the UAV group or determining their location coordinates. Therefore, the influence of the accuracy of the distance measurement between individual group members on the accuracy of determining the location coordinates of individual UAVs was investigated. Errors in determining the position of a member of a group of UAVs are mainly affected by the geometric configuration of the communication network users, the quality of the parameters transmitted in the FOs position report, and the network synchronization. These factors can significantly affect the accuracy of measuring the distance, D_{1-4}, between individual group members and the group leader. The distance measurement errors, Δd_{i-v}, where i = 1, 2, 3, 4, will be modeled with a random number generator with a normal distribution. The generated random numbers will be added to the actual coordinates of the UAVs, ZP_i, i = 1 to 4. The parameters of the normalized normal distribution are E (x) = m = 0 is the mean, and the variance is V (x) = σ^2 = 1. Since we had 4 UAVs in the group, we needed 12 random number generators. The magnitude of the error of each coordinate was varied using the constant k, by which we multiplied each generated random number, where:

$$M[k.X] = k. \, M. \, [X], \tag{34}$$

$$D[c.X] = c^2 .D[X], \tag{35}$$

where: M—mean value, D—dispersion, k—non-random variable (constant), and X—random variable.

The errors were written to the row matrix for each coordinate and each user, separately:

$$\Delta X_{ZP\_i} = [\Delta x_1^i, \Delta x_2^i, ..., \Delta x_n^i], \tag{36}$$

$$\Delta Y_{ZP\_i} = [\Delta y_1^i, \Delta y_2^i, ..., \Delta y_n^i], \tag{37}$$

$$\Delta Z_{ZP\_i} = [\Delta z_1^i, \Delta z_2^i, ..., \Delta z_n^i], \tag{38}$$

where: i = 1, 2, 3, 4,

n is the number of simulation steps,

ΔX_{ZP_i}—row matrix of randomly generated errors of the x coordinate of user $ZP_{\_i}$,

ΔY_{ZP_i}—row matrix of randomly generated errors of y coordinate of user ZP_i,

ΔZ_{ZP_i}—row matrix of randomly generated errors of z coordinate of user ZP_i.

Using the scalar sum operation of matrix elements 2 and matrix elements 30 to 32, we obtained new row matrices, the elements of which will represent the X, Y, and Z coordinates of each PZ_i, with errors.

$$X_{ZP\_ic} = X_{ZP\_i} + \Delta X_{ZP\_i} = [x_1^i + \Delta x_1^i, x_2^i + \Delta x_2^i, ..., x_n^i + \Delta x_n^i], \tag{39}$$

$$Y_{ZP\_ic} = Y_{ZP\_i} + \Delta Y_{ZP\_i} = [y_1^i + \Delta y_1^i, y_2^i + \Delta y_2^i, ..., y_n^i + \Delta y_n^i], \tag{40}$$

$$Z_{ZP\_ic} = Z_{ZP\_i} + \Delta Z_{ZP\_i} = [z_1^i + \Delta z_1^i, z_2^i + \Delta z_2^i, ..., z_n^i + \Delta z_n^i], \tag{41}$$

where:

X_{ZP_ic}—row matrix of coordinate X of user ZP_i with error Δx^i,

Y_{ZP_ic}—row matrix of coordinate Y of user ZP_i with error Δy^i,

Z_{ZP_ic}—row matrix of coordinate Z of user ZP_i with error Δz^i.

To calculate the pseudo-range between individual UAVs and the group commander, the geocentric coordinates from (2) and (13)–(16) and the coordinate errors of UAVs from matrices (33) to (35) will be used. From Relationship (7), the equation for calculating the pseudo-range, di, was obtained:

$$d_i = \sqrt{\left(x^5_{1...n} - (x^i_{1...n} + \Delta x^i_{1...n})\right)^2 + \left(y^5_{1...n} - (y^i_{1...n} + \Delta y^i_{1...n})\right)^2 + \left(z^5_{1...n} - (z^i_{1...n} + \Delta z^i_{1...n})\right)^2} \quad (42)$$

where: i = 1, 2, 3, 4 (user index), and $x^5_{1...n}$, $y^5_{1...n}$, and $z^5_{1...n}$ are the x, y, and z coordinates of the group commander UAV.

The distance measurement error, Δdi, is as follows:

$$\Delta d_i = D_i - d_i \quad (43)$$

where D_i is the actual distance between individual UAVs and the group commander, and d_i is the calculated pseudo-distance between individual UAVs and the group commander.

The flight simulation flow diagram of a group of UAVs and the determination of the position of the group leader is shown in Figure 8. After entering the initial flight conditions, the flight trajectory of the group of UAVs was calculated and displayed. Subsequently, errors were generated in determining the coordinates of the four members of the group of UAVs and in measuring the distance between the individual UAVs and the group commander. The generated errors were added to the flight coordinates of the UAVs, and the position of the group leader was calculated. Based on the comparison of the calculated position of the group commander with the simulated trajectory of its flight, the errors in determining its position were determined. Then, these errors were recorded graphically.
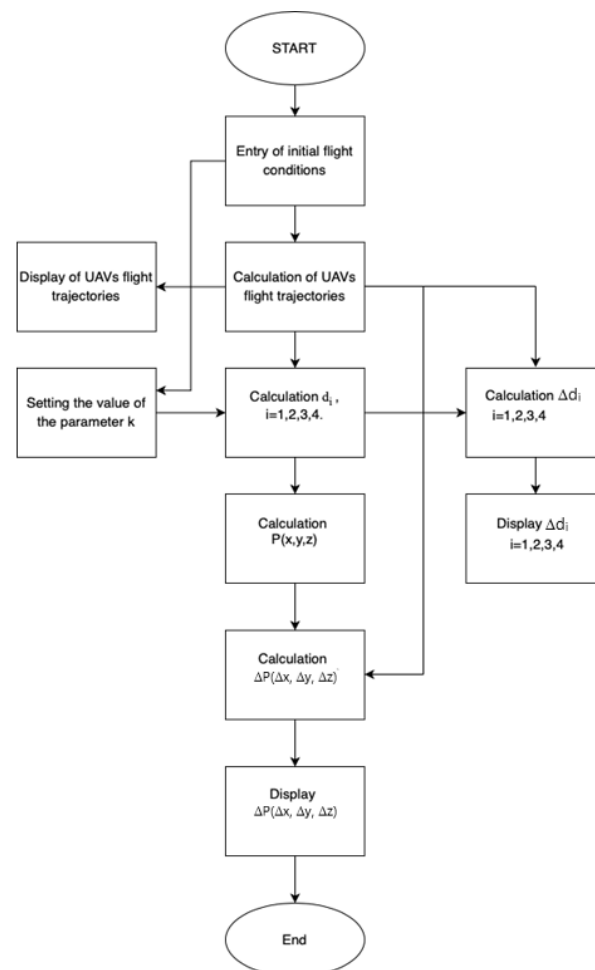

Figure 8. The flight simulation flow diagram of a group of UAVs.

3. Discussion and Results of the Evaluation Accuracy of Determination of the Positioning of the Group Commander

To verify the sensitivity of the proposed equations to inaccuracies in measuring the distance between individual UAVs and the group commander, we performed several simulations using the flight model of a group of UAVs, as described in the second section (see Figure 3). The flight trajectory consisted of a straight flight and three turns. The initial coordinates of the FOs are provided in Table 1. Initial conditions for the UAV flight models are presented in the first section. Distance measurement errors between individual UAVs and the group commander were simulated using Relations (34)–(43). The magnitude of the distance measurement inaccuracy was changed using the constant k by the Relations (34) and (35). The constant k in the range from **0.0 to 1.0** will be changed. The simulation results are shown in Figures 9–16. Errors in determining the group commander's coordinates are shown in blue, and errors in determining the group commander's position are shown in red.

Figure 9. Distance measurement errors between individual UAVs and the group commander for k = 0.0.
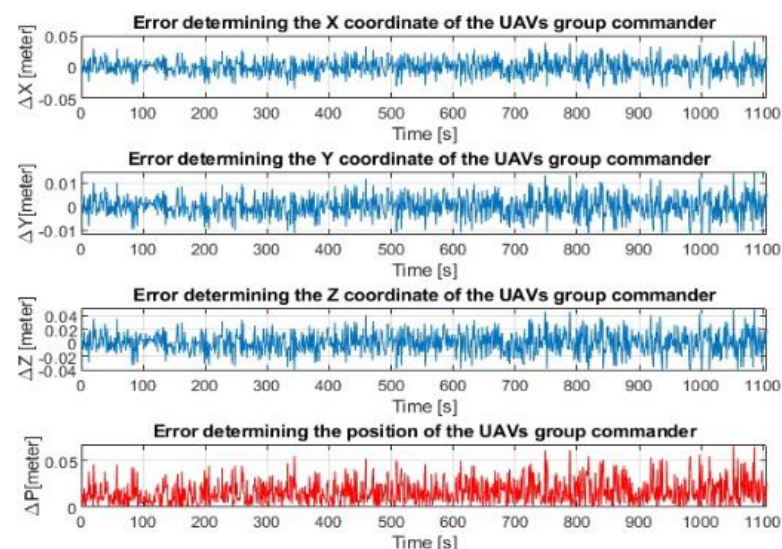

Figure 10. Errors in determining the coordinates of the position of the commander of the group of UAVs.
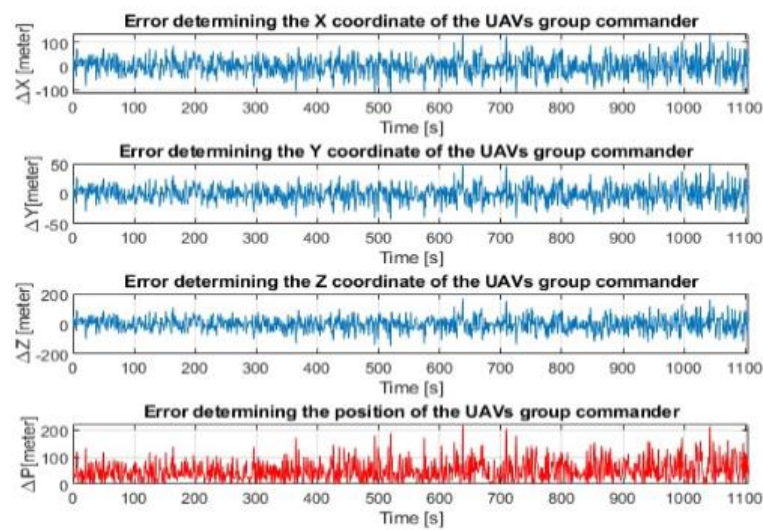
Figure 11. Errors in determining the coordinates and position of the UAV group commander for k = 0.01.
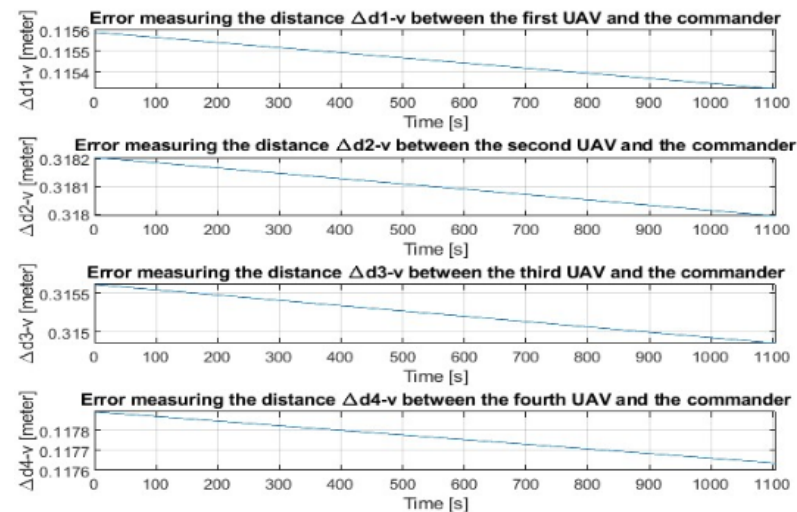

Figure 12. Distance measurement errors between individual UAVs and the group commander for k = 0.5.
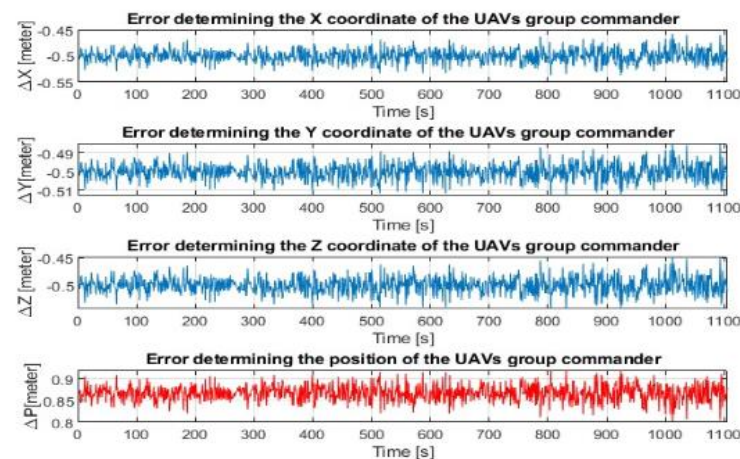

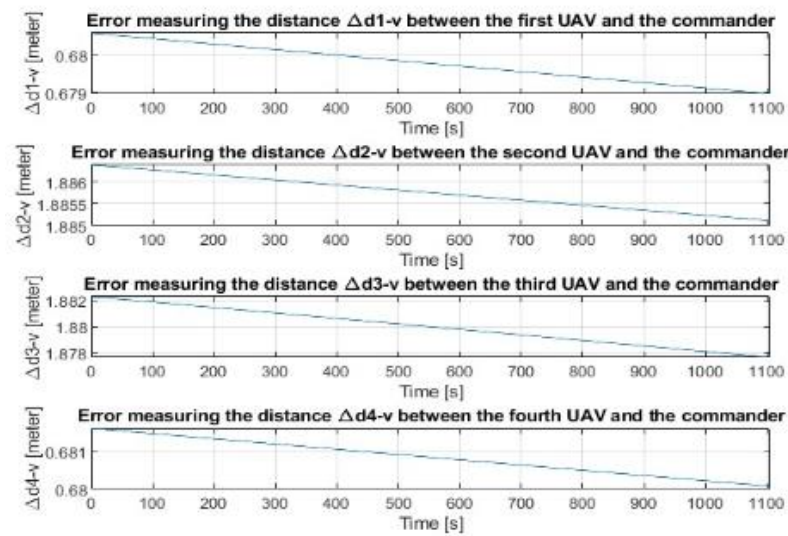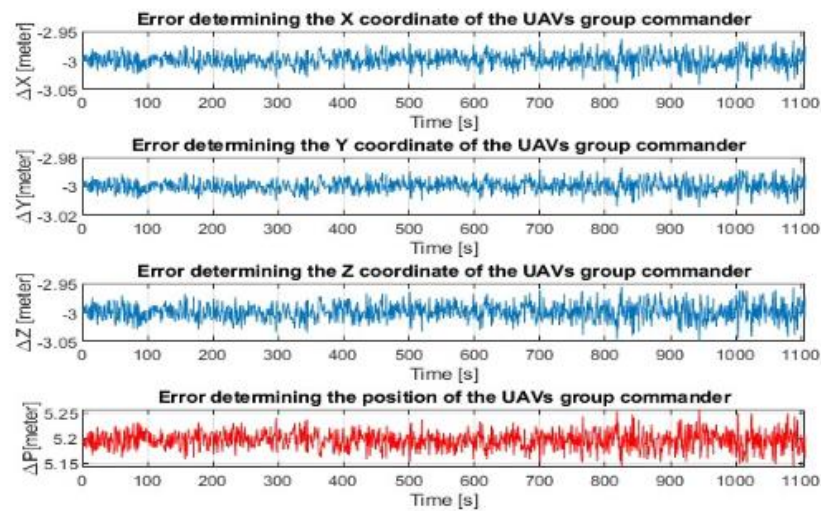**Figure 13.** Errors in determining the coordinates and position of the UAV group commander for k = 0.5.

Figure 14. Distance measurement errors between individual UAVs and the group commander for k = 3.0.

Figure 15. Errors in determining the coordinates and position of the UAV group commander for k = 3.0.
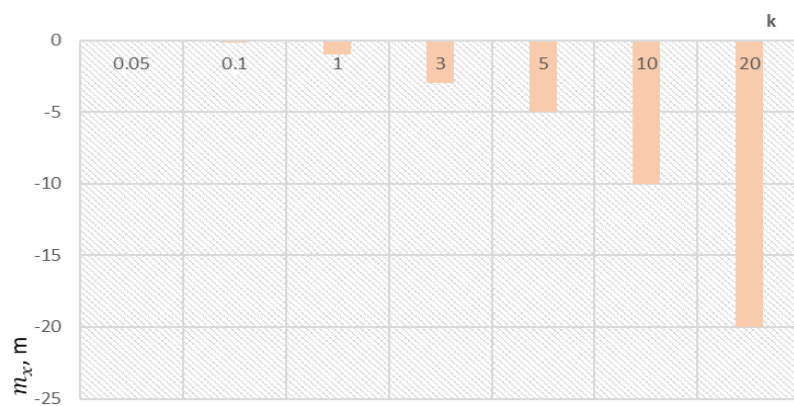

Figure 16. The mean values of group commander x coordinate determination errors m_x, for the constant k = 0.05 to 20.

First, we checked the accuracy of determining the group commander's position using the telemetry method during the group's flight according to the scenario shown in Figure 3.

We assumed that we knew the exact distances between the group commander and the individual UAVs and the exact positions of the individual members of the group. In this case, the constant k was equal to zero. The simulation results are shown in Figures 9 and 10.

Figure 9 clearly shows that we knew the exact distances between the group commander and the individual UAVs. Therefore, the distance measurement errors were zero. In this simulation, we assumed that we knew the exact positions of the individual UAVs.

Despite this, the errors in determining the coordinates and position of the group commander were different from zero. The mean value of the error when determining the position of the group commander was equal to 0.044 m and the dispersion was equal to 2.9 m^2. We consider these errors to be methodological errors of the proposed method. We investigated the effect that inaccuracies in determining the coordinates of individual UAVs and errors in measuring the distance between individual UAVs and the group commander will have on determining the position of the group commander. The constant k was equal to 0.01. Therefore, we simulated errors in determining the coordinates of individual UAVs and errors in measuring the distance between individual UAVs and the group commander by Equations (34)–(43). The coordinate and distance determination errors were random for each UAV.

The simulation results are shown in Figure 11. The simulation results clearly showed that even small errors in determining the coordinates of individual UAVs and measuring the distance between them and the group commander significantly impacted the accuracy of determining its position. This can be explained by the fact that errors in determining the position of four points in space and errors in determining the distance of these points from the position of an unknown point in space, whose position we want to calculate, have a significant impact on the calculation of the position of this unknown point. Based on the results, we investigated how the accuracy of determining the position of the group commander will change during the flight when the errors of determining the coordinates of individual UAVs are the same. Using the constant k, we varied the size of the coordinate errors. The results of these simulations are shown in Figures 12–16.

Figure 12 shows the distance measurement errors between individual UAVs and the group commander for k = 0.5. The figure shows that the distance measurement errors for k = 0.5 varied from 0.11 m to 0.31 m during the UAVs' flight. As can be seen from Figure 13, errors in determining the coordinates of individual UAVs and errors in measuring the distance between individual UAVs and the group commander caused errors in determining the position of the group commander's position. For k = 0.5, the mean value of the error of determining the commander's position was equal to 0.87 m, and the dispersion was 0.47 m^2. Next, we performed a simulation for the constant k = 3.0. In this case, the errors in measuring the distance between the individual UAVs and the group commander were from 0.67 m to 1.88 m (see Figure 14).

As can be seen from Figure 15, bigger errors in determining the coordinates of individual UAVs and errors in measuring the distance between individual UAVs and the group commander caused bigger errors in determining the group commander's position. For k = 3.0, the mean value of the error of determining the commander's position was equal to 5.22 m, and the dispersion was 14.1 m^2.

In this way, we gradually checked the influence of the inaccuracy in determining the coordinates of individual UAVs and distance measurement errors between individual UAVs and the group commander for the constant k, equal to 0.05 to 20, which corresponded to distance measurement errors from 0.01 to 12.0 m. The simulation results are presented in Figures 16–19. Figure 16 shows the mean values of the errors of determining the coordinate x group commander m_x for the constant k = 0.05 to 20. The mean values of the errors of determining the coordinate x group commander ranged from −0.05 m to −20.0 m.
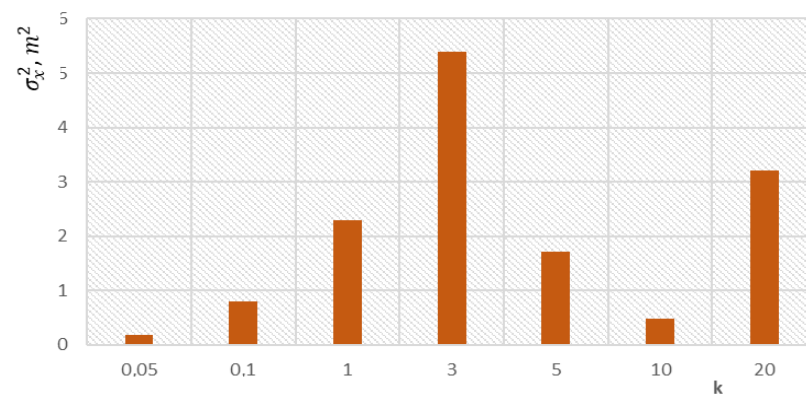
Figure 17. The variance of group commander x coordinate determination errors, σ^2_x, for the constant $k = 0.05$ to 20.
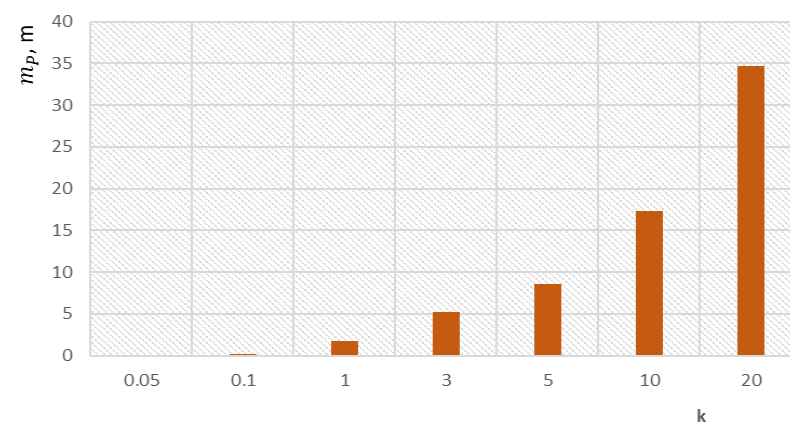

Figure 18. The mean values of group commander m_p position determination errors for the constant $k = 0.05$ to 20.
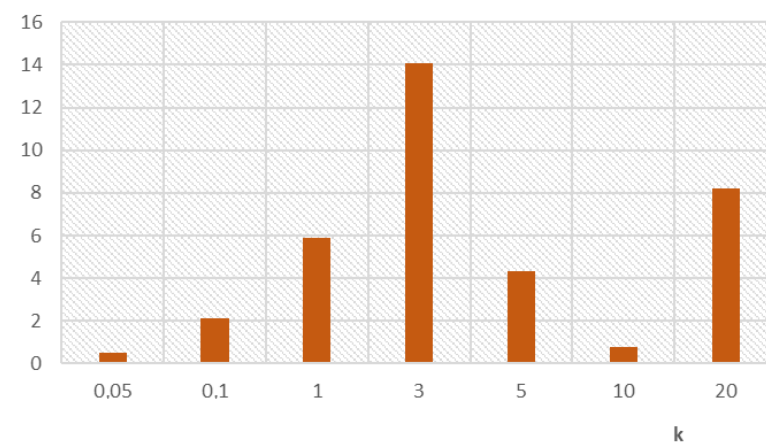

Figure 19. The dispersion of group commander σ^2_p positioning errors for the constant $k = 0.05$ to 20.

Figure 17 shows the variance of group commander x coordinate determination errors, σ^2_x, for the constant $k = 0.05$ to 20. The group commander x coordinate determination error variance values ranged from 0.19 m^2 to 5.4 m^2.

The simulation results confirmed that when the constant k changed from 0 to 20, the errors in determining the group commander's coordinates y and z changed in approximately the same range as the errors in determining the group commander's coordinate x. Figure 18 shows the mean values of group commander m_p position determination errors for the

constant k = 0.05 to 20. The mean values of group commander position determination errors ranged from 0.11 m to 34.65 m.

Figure 19 shows the dispersion of the group commander σ^2_p positioning errors for the constant k = 0.05 to 20. The GC positioning error dispersion values ranged from 0.5 m^2 to 14.1 m^2.

The simulation results confirmed that when the constant k changed from 0 to 20, the errors of determining the coordinates y and z of the group commander changed in approximately the same range as the errors of determining the coordinate x of the group commander. The simulation results showed that if the errors in determining the coordinates of the members of the group of UAVs increased, then the errors in determining the coordinates of the group commander increased. The accuracy of determining the position of the group commander was also influenced by the accuracy of determining the distance between individual UAVs and the group commander. When the constant k was increased, the errors in determining the position of the group commander increased. Based on this, we can conclude that for accurate determination of the position of the group commander, the errors in measuring the distance between individual UAVs and the group commander must be less than 1.9 m.

4. Conclusions

Developments in the field of UAVs confirm that these systems have great application possibilities. Among the main areas of their use are terrain control in agriculture, object monitoring, and recently, reconnaissance and attack missions in the military. The main advantages of their operation include their affordable price, multiple uses, and the possibility of autonomous operation in certain areas. In this work, we created a flight model of five UAVs in the geocentric coordinate system, which fly in a specified formation. The assembly of the UAVs consisted of a commander and four other UAVs. The technical data of the General Atomics MQ-9 Reaper UAV set the parameters of the created models. The simulation confirmed that the developed models simulated UAV flight trajectories consisting of a straight section and three turns. An equation for determining the position of a selected member of a group of UAVs was created, provided that the group had its own telecommunications network. The following prerequisites must be met in this network. Each network user has a precisely determined time for sending messages, which must contain information about its location. Based on this, it is possible to determine the distances between users, and each user can determine their position. All simulations were performed using MATLAB software. A simulation was constructed to determine the position of the commander of the group of UAVs, assuming that we knew the exact positions of the individual UAVs and the distances between them and the commander of the group. The results confirmed that, under the mentioned conditions, it is possible to determine the group commander's position accurately. Next, we performed a simulation to determine the position of the commander of the group of UAVs, assuming that the group flew in a specified formation. The simulation confirmed that the errors in determining the coordinates of the group commander's position differed from zero. The mean value of the error in determining the position of the group commander was equal to 0.044 m, and the variance was equal to 2.9 m^2. We consider these errors to be methodological errors of the proposed method. Based on the results, we investigated how the accuracy of determining the position of the group commander will change during the flight when the errors in determining the coordinates of individual UAVs are the same. The magnitude of these errors was varied using the constant k. When changing the constant k from 0 to 20, the errors in determining the coordinates of the group commander varied from 0.11 m to 34.6 m. The simulation results showed that if the errors in determining the coordinates of the members of the group of UAVs increased, then the errors in determining the coordinates of the group commander increased. The accuracy of determining the position of the group commander was also influenced by the accuracy of determining the distance between individual UAVs and the group commander. The simulation results showed that to accurately determine the

group commander's position, the distance measurement errors between individual UAVs and the group commander must be less than 1.9 m. To compare our results with other works, we present two examples. In [3], the authors solved the problems of cooperative control of UAVs. They reported that the relative distance error between two UAVs and the stationary goal was around 270.0 m. The problem of controlling UAV maneuvering while tracking the target and avoiding obstacles on the route using a method based on the deep deterministic policy gradient was solved in [4]. In this case, the distance error between the UAV and the target was 300.0 m to 0.0 m. The research results showed that the telemetry method can be used to determine the position of individual members of the UAV group. Based on this, it is possible to control the flight of individual group members so that they adhere to the selected set-up. The advantage of this method is that it does not require the reception of signals from satellite navigation systems, which can be interfered with under certain conditions. Our further research will focus on improving the signal processing equations of participants working in the telecommunications network so that they are not overly sensitive to errors in measuring the distance between individual participants nor to inaccuracies in entering the location of individual network participants.

References

1. Huang, G.; Hu, M.; Yang, X.; Lin, P. Multi-UAV Cooperative Trajectory Planning Based on FDS-ADEA in Complex Environments. *Drones* **2023**, *7*, 55. [CrossRef]
2. Li, B.; Gan, Z.; Chen, D.; Aleksandrovich, S. UAV Maneuvering Target Tracking in Uncertain Environments Based on Deep Reinforcement Learning and Meta-Learning. *Remote Sens.* **2020**, *12*, 3789. [CrossRef]
3. Zhang, J.; Yan, J.; Zhang, P.; Kong, X. Design and Information Architectures for an Unmanned Aerial Vehicle Cooperative Formation Tracking Controller. *IEEE Access* **2018**, *6*, 45821–45833. [CrossRef]
4. Li, B.; Yang, Z.P.; Chen, D.Q.; Liang, S.Y.; Ma, H. Maneuvering target tracking of UAV based on MN-DDPG and transfer learning. *Def. Technol.* **2021**, *17*, 10. [CrossRef]
5. Li, Y.; Tian, B.; Yang, Y.; Li, C. Path planning of robot based on artificial potential field method. In Proceedings of the 2022 IEEE 6th Information Technology and Mechatronics Engineering Conference (ITOEC), Chongqing, China, 4–6 March 2022; pp. 91–94.
6. Zong, C.; Yao, X.; Fu, X. Path Planning of Mobile Robot based on Improved Ant Colony Algorithm. In Proceedings of the 2022 IEEE 10th Joint International Information Technology and Artificial Intelligence Conference (ITAIC), Chongqing, China, 17–19 June 2022; pp. 1106–1110.
7. Gao, Y. An Improved Hybrid Group Intelligent Algorithm Based on Artificial Bee Colony and Particle Swarm Optimization. In Proceedings of the 2018 International Conference on Virtual Reality and Intelligent Systems (ICVRIS), Hunan, China, 10–11 August 2018; pp. 160–163.
8. Sahu, A.; Kandath, H.; Krishna, K.M. Model predictive control based algorithm for multi-target tracking using a swarm of fixed wing UAVs. In Proceedings of the 2021 IEEE 17th International Conference on Automation Science and Engineering (CASE), Lyon, France, 23–27 August 2021; pp. 1255–1260.
9. Wang, D.; Wu, M.; He, Y.; Pang, L.; Xu, Q.; Zhang, R. An HAP and UAVs Collaboration Framework for Uplink Secure Rate Maximization in NOMA-Enabled IoT Networks. *Remote Sens.* **2022**, *14*, 4501. [CrossRef]
10. Wang, D.; He, T.; Zhou, F.; Cheng, J.; Zhang, R.; Wu, Q. Outage-driven link selection for secure buffer-aided networks. *Sci. China Inf. Sci.* **2022**, *65*, 182303. [CrossRef]
11. Hu, X.; Cheng, J.; Zhou, M.; Hu, B.; Jiang, X.; Guo, Y.; Bai, K.; Wang, F. Emotion-aware cognitive system in multi-channel cognitive radio ad hoc networks. *IEEE Commun. Mag.* **2018**, *56*, 180–187. [CrossRef]
12. Nie, Z.; Zhang, X.; Guan, X. UAV formation flight based on the artificial potential force in 3D environment. In Proceedings of the 2017 29th Chinese Control and Decision Conference (CCDC), Chongqing, China, 28–30 May 2017; pp. 5465–5470.

13. Cetin, O.; Yilmaz, G. Real-time autonomous UAV formation flight with collision and obstacle avoidance in the unknown environment. *J. Intell. Robot. Syst.* **2016**, *84*, 415–433. [CrossRef]

14. Ming, Z.; Lingling, Z.; Xiaohong, S.; Peijun, M.; Yanhang, Z. Improved Discrete Mapping Differential Evolution for Multi-Unmanned Aerial Vehicles Cooperative Multi-Targets Assignment under Unified Model. *Int. J. Mach. Learn. Cybern.* **2017**, *8*, 765–780. [CrossRef]

15. Chai, X.; Zheng, Z.; Xiao, J.; Yan, L.; Qu, B.; Wen, P.; Wang, H.; Zhou, Y.; Sun, H. Multi-Strategy Fusion Differential Evolution Algorithm for UAV Path Planning in Complex Environment. *Aerosp. Sci. Technol.* **2022**, *121*, 107287. [CrossRef]

16. Sun, X.; Zhang, B.; Chai, R.; Tsourdos, A.; Chai, S. UAV Trajectory Optimization Using Chance-Constrained Second-Order Cone Programming. *Aerosp. Sci. Technol.* **2022**, *121*, 107283. [CrossRef]

17. Beinarovica, A.; Gorobetz, M.; Levchenkov, A. The control algorithm of multiple unmanned electrical aerial vehicles for their collision prevention. In Proceedings of the 12th International Conference on Intelligent Technologies in Logistics and Mechatronics Systems (ITELMS), Panevezys, Lithuania, 26–27 April 2018; pp. 37–43.

18. Graffstein, J. Functioning of an air anti-collision system during the test flight. *Aviation* **2014**, *18*, 44–51. [CrossRef]

19. Zhao, W.; Li, L.; Wang, Y.; Zhan, H.; Fu, Y.; Song, Y. Research on A Global Path-Planning Algorithm for Unmanned Arial Vehicle Swarm in Three-Dimensional Space Based on Theta*–Artificial Potential Field Method. *Drones* **2024**, *8*, 125. [CrossRef]

20. Zhang, S.; Xu, M.; Wang, X. Research on Obstacle Avoidance Algorithm of Multi-UAV Consistent Formation Based on Improved Dynamic Window Approach. In Proceedings of the 2022 IEEE Asia-Pacific Conference on Image Processing, Electronics and Computers (IPEC), Dalian, China, 14–16 April 2022; pp. 991–996.

21. Jing, X.; Hou, M.; Wu, G.; Ma, Z.; Tao, Z. Research on maneuvering decision algorithm based on improved deep deterministic policy gradient. *IEEE Access* **2022**, *10*, 92426–92445.

22. Fujimoto, S.; Hoof, H.; Meger, D. Addressing function approximation error in actor-critic methods. In *International Conference on Machine Learning*; PMLR: New York, NY, USA, 2018; pp. 1587–1596.

23. Zhang, S.; Li, Y.; Dong, Q. Autonomous navigation of UAV in multiobstacle environments based on a Deep Reinforcement Learning approach. *Appl. Soft Comput.* **2022**, *115*, 108194. [CrossRef]

24. Zhang, H.; Huang, C.; Xuan, Y.; Tang, S. Maneuver decision of autonomous air combat of un-manned combat aerial vehicle based on deep neural network. *Acta Armamentaria* **2020**, *41*, 1613–1622.

25. Luo, Y. *Research on Air Combat Decision Method Based on Dynamic Bayesian Network*; Shenyang Aerospace University: Shen Yang, China, 2018; pp. 1–62.

26. Dzunda, M.; Dzurovcin, P.; Melniková, L. Determination of Flying Objects Position. In *TransNav: The International Journal on Marine Navigation and Safety of Sea Transportation*; Vol. 13 No.2-june 2019; Faculty of Navigation: Gdyňa, Poľsko, 2019; pp. s423–s428.

27. Džunda, M.; Kotianová, N.; Dzurovčin, P.; Szabo, S.; Jenčová, E.; Vajdová, I.; Košcák, P.; Liptáková, D.; Hanák, P. Selected Aspects of Using the Telemetry Method in Synthesis of RelNav System for Air Traffic Control. *Int. J. Environ. Res. Public Health* **2020**, *17*, 213. [CrossRef] [PubMed]